Skeletal Radiol (2011) 40:1587–1594
DOI 10.1007/s00256-011-1208-1

TECHNICAL REPORT

Oblique axial MR imaging of the normal anterior cruciate ligament bundles

Alex Wing Hung Ng · James F. Griffith · Kan Yip Law · James W. M. Ting · George L. Tipoe · Anil T. Ahuja · Kai Ming Chan

Received: 27 March 2011 / Revised: 12 May 2011 / Accepted: 12 May 2011 / Published online: 4 June 2011

Introduction

The anterior cruciate ligament (ACL) is composed of the anteromedial and posterolateral bundles [1, 2]. Although these two bundles are closely aligned anatomically, they do have distinct biomechanical functions with the anteromedial bundle stabilizing the knee in flexion and the posterolateral bundle stabilizing the knee in extension [1–5].

A. W. H. Ng (✉) · J. F. Griffith · A. T. Ahuja
Department of Imaging and Interventional Radiology,
Prince of Wales Hospital, Chinese University of Hong Kong,
30-32 Ngan Shing Street, Shatin, N.T.,
Hong Kong SAR, Hong Kong
e-mail: alex@sunghim.com

J. F. Griffith
e-mail: griffith@cuhk.edu.hk

A. T. Ahuja
e-mail: ahujaa@ha.org.hk

K. Y. Law · K. M. Chan
Department of Orthopedics and Traumatology,
Prince of Wales Hospital, Chinese University of Hong Kong,
Hong Kong, Hong Kong

K. Y. Law
e-mail: kylaw@ort.cuhk.edu.hk

K. M. Chan
e-mail: kaimingchan@cuhk.edu.hk

J. W. M. Ting · G. L. Tipoe
Department of Anatomy, University of Hong Kong,
Hong Kong, Hong Kong

J. W. M. Ting
e-mail: jwmting@hkucc.hku.hk

G. L. Tipoe
e-mail: tgeorge@hkucc.hku.hk

Most ACL tears are complete with the tear extending across both bundles. Partial tears of the ACL are less frequently encountered and may involve both bundles to a similar degree or one bundle predominantly. Although complete ACL tears do not have the capacity to heal, a limited blood supply to the ACL via the medial geniculate artery does allow healing of partial tears [6, 7]. Correct assessment regarding the presence, severity, and location of partial tears is relevant since delayed recognition of a partial tear can result in progression to complete tear [6]. Also, if only one bundle is predominantly torn, isolated single bundle reconstruction rather than full ACL graft reconstruction may be undertaken [8, 9]. Early evaluation of partial ACL tears could possibly improve clinical and surgical management [10].

A prerequisite to diagnosing ACL bundle injury on MR imaging is clear delineation of both bundles and awareness of their normal appearance. Orthogonal planes can delineate the normal ACL bundle structure in only 42% of knees [11]. In this study, we describe a new oblique axial plane for imaging the normal ACL bundles on MR imaging; evaluate how well the normal ACL bundles can be evaluated on this plane compared to the standard sagittal, coronal, and axial planes [12–15]; and describe the normal MR appearances.

Materials and methods

Subjects

Signed informed consent was obtained from all participating subjects with the study protocol first being approved by the Institutional Ethics committee. A total of 60 knees (34 males, 26 females; mean age 37.1 years; range 13–73 years)

with a normal ACL were studied to help establish the normal appearances of the ACL on oblique axial MR imaging between September 2009 and June 2010. These subjects included 20 healthy volunteers with no knee symptoms or injury. In addition, 40 subjects without history of knee injury referred from the Orthopaedic Department for MR knee examination for knee pain were studied. These participating subjects were assessed by experienced orthopedic surgeons, and no clinical features of knee laxity were found.

MR protocol

MR examinations were performed on a 3 T imaging system (Philips X-series, Best, Netherlands) using a phased array knee coil with eight elements. The knee was examined in a supine and extended position. Knee examination comprised (1) turbo-spin-echo sagittal intermediate-weighted imaging (TR=3,000 ms, TE=30 ms, bandwidth=291 Hz, TSE factor=10, 3 mm slice thickness, interslice gap=0.3 mm, voxel size=0.40×0.54 mm, NEX=2, FOV=160 mm), planned in a plane parallel to the outer cortex of the lateral femoral condyle, (2) coronal T2-weighted fat suppression imaging (TR=2,800 ms, TE=60 ms, bandwidth=268 Hz, TSE factor=12, 3 mm slice thickness, interslice gap=0.3 mm, voxel size=0.50×0.67 mm, NEX=2, FOV=160 mm), and (3) axial intermediate-weighted fat-suppressed imaging (TR=3,000 ms, TE=30 ms, bandwidth=218 Hz, TSE factor=14, 3 mm slice thickness, interslice gap=0.3 mm, voxel size=0.45×0.56 mm, NEX=2, FOV=150 mm) followed by (4) oblique axial imaging of the ACL. Oblique axial imaging of the ACL comprised intermediate-weighted (TR=3,000 ms, TE=30 ms, 3 mm slice thickness, interslice gap=0.3 mm, bandwidth=328 Hz, TSE factor=13, voxel size=0.25×0.31 mm, NEX=2, FOV=120 mm) images obtained in a plane aligned perpendicular to the course of the ACL using sagittal and coronal images for positioning and alignment (Fig. 1). This extra sequence took approximately 4 min to complete.

MR image analysis

Two staff radiologists (AWH Ng and JF Griffith; with 15 years and 24 years of MR musculoskeletal reporting experience, respectively) independently reviewed oblique axial and standard sagittal, coronal, and axial image datasets of different subjects in random order. Analysis was performed at a Digital Imaging and Communications in Medicine Viewer (OsiriX viewer). The ability to delineate the anteromedial and posterolateral bundles of the ACL near the tibial insertion, the mid-portion, and near the femoral origin was assessed. Bundle delineation was classified as good, adequate, or poor. Good delineation indicated unequivocal delineation of both bundle outlines, adequate delineation indicated delineation of both bundle outlines with a moderate degree of confidence, while poor delineation reflected a situation where both bundle outlines could not be separated with confidence (Fig. 2).

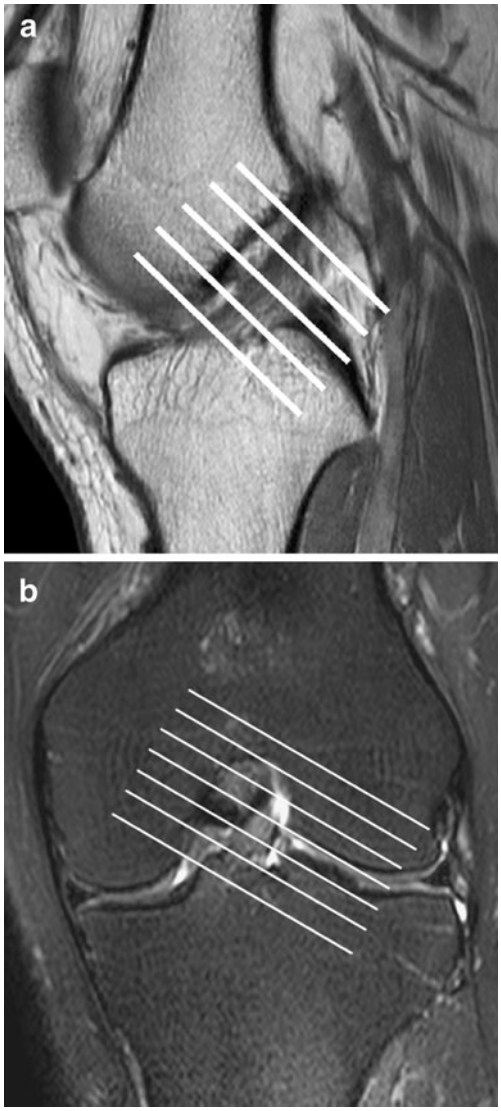

Fig. 1 Oblique intermediate-weighted axial imaging of the ACL was planned using both **a** standard sagittal intermediate-weighted images (*white lines*) and **b** standard coronal T2-weighted fat suppression (*white lines*). It can also be planned using analogous scout views

The typical appearance of ACL was defined as the appearance of both bundles commonly found in the majority of oblique axial images at the three levels. The presence of additional structures such as an intermediate bundle, ligamentum mucosum, and ganglion cysts was also recorded.

Correlative anatomical sectioning of cadaveric knee

Intermediate-weighted oblique axial imaging of the ACL was performed on a single embalmed cadaveric knee. The

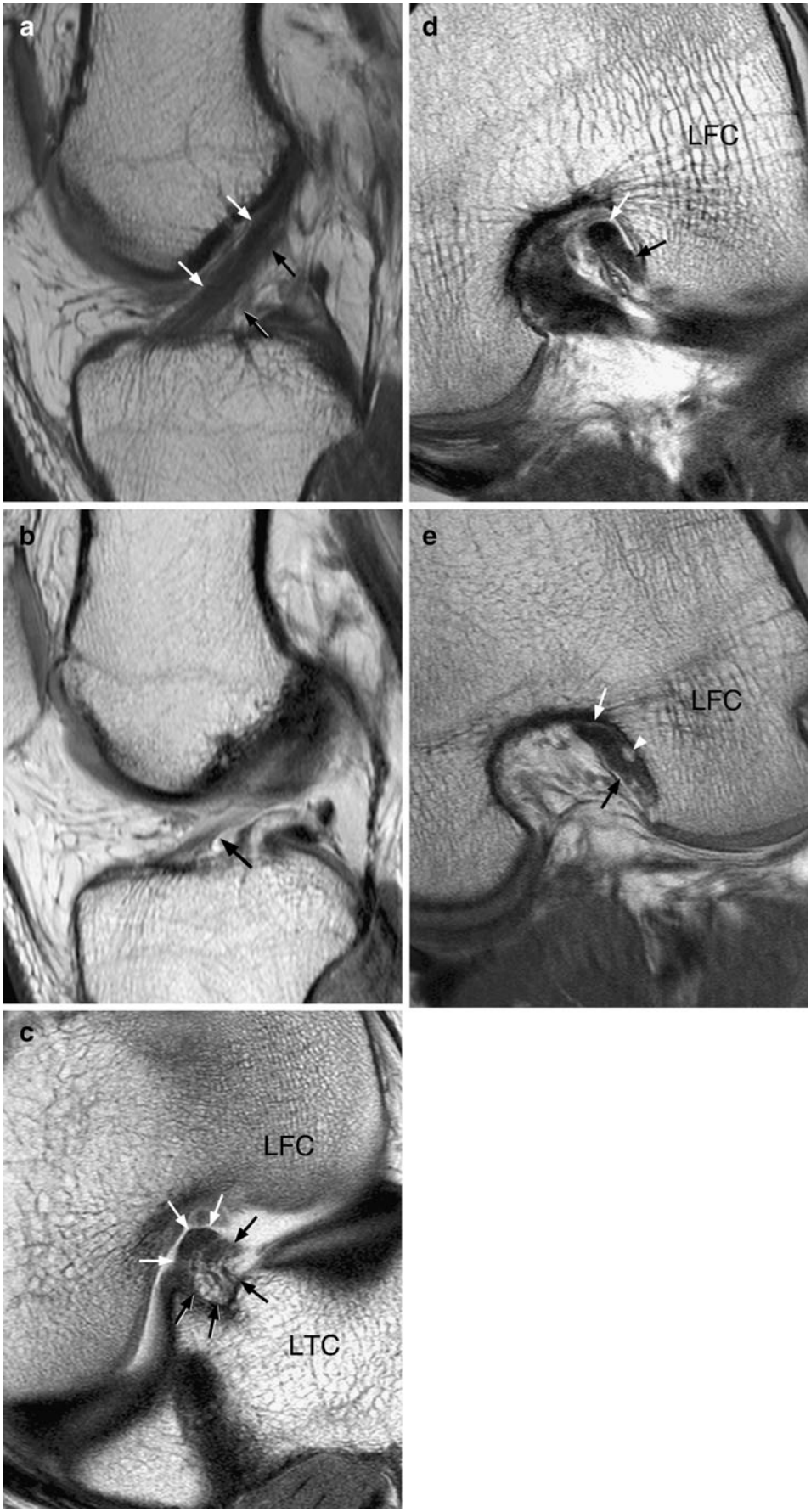

Fig. 2 **a**–**b** Two consecutive intermediate-weighted sagittal images of the ACL in this example were graded as adequate near the tibial insertion, poor in the mid-portion, and poor near the femoral origin. **c**–**e** Oblique intermediate-weighted axial images of the ACL in three different locations were all graded as good near the tibial origin (**b**), good at the mid-portion (**c**), and good at the femoral origin (**d**). There is an incidental finding of a small ganglion cyst (*white arrowhead*) within the posterolateral bundle close to the femoral origin that was confirmed on the fat suppression sequence (not shown). Anteromedial bundle (*white arrows*). Posterolateral bundle (*black arrows*). *LFC* Lateral femoral condyle, *LTC* lateral tibial condyle

ACL was shown to be normal on MR examination. Using MR planning, this specimen was sectioned with a bandsaw into contiguous 3–4 mm anatomical sections along an oblique axial plane orthogonal to the ACL. Conventional photographs of these anatomical sections were obtained.

Statistical analysis

The ability to delineate the two bundles in oblique axial and standard sagittal, coronal, and axial views was compared using the Wilcoxon signed rank test as was the relationship among age, gender, and bundle delineation. A P value of less than 0.05 indicated a statistically significant difference. Cohen weighted k statistic was used to assess the level of interobserver agreement with regard to delineation of the ACL bundles. A value of less than 0.20 implied poor agreement; values of 0.21–0.40, fair agreement; values of 0.41–0.60, moderate agreement; values of 0.61–0.80, substantial agreement; and values of 0.81–1.00, almost perfect agreement [16].

Results

Delineation of the individual ACL bundles was not related to age or gender ($P>0.05$).

Typical appearances of normal ACL on intermediate-weighted oblique axial imaging

Typical appearances of the ACL were present in 49 (82%) of 60 knees examined. At all levels, the anteromedial bundle was located at the anteromedial aspect of the ACL, while the posterolateral bundle was located more posterolaterally. Close to the tibial insertion, 95% (57 out of 60) of anteromedial bundles comprised a thick C-shaped hypointense rim with a central hyperintense area (Fig. 3). The posterolateral bundle comprised a more loosely arranged conglomeration of ligament fibres separated by fatty-type tissue. At the mid-portion of the ACL, both the anteromedial and posterolateral bundles become more compact and rounded in appearance (Fig. 4), while near the femoral attachment both bundles become more oblong in contour with the anteromedial bundle being typically uniformly hypointense and the posterolateral bundle slightly less hypointense (Fig. 5). Correlative anatomical sections of a cadaveric knee at these three levels are shown (Figs. 3, 4, 5).

Atypical appearances of ACL on oblique axial imaging in normal subjects

Atypical appearances were present in 11 (18%) of 60 knees examined as follows.

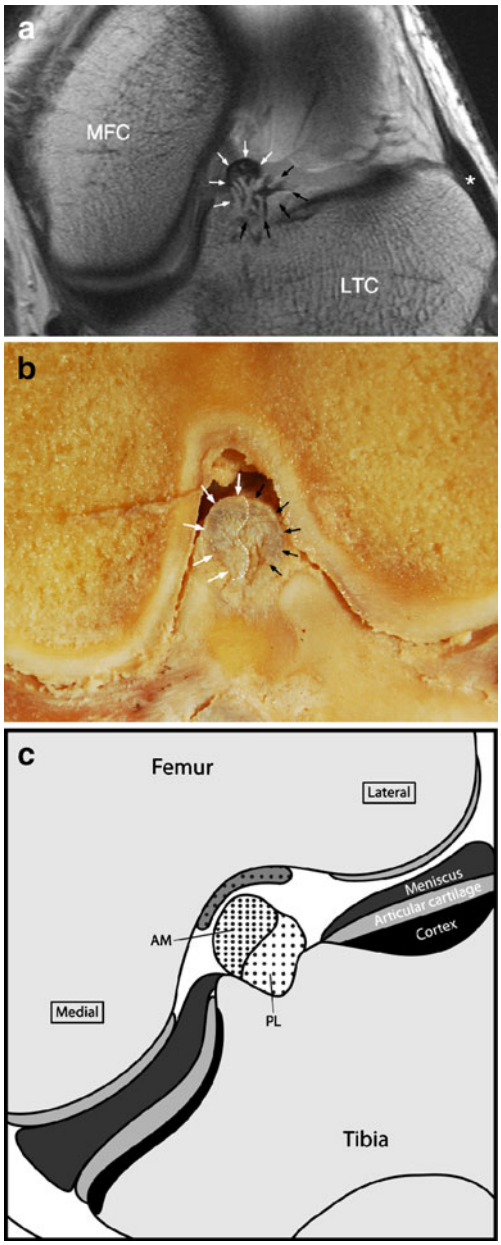

Fig. 3 **a** Oblique intermediate-weighted axial imaging of ACL near the tibial insertion in a volunteer. The anteromedial bundle (*white arrows*) comprises a C-shaped hypointense rim with a central fatty-type area and originates from the anteromedial aspect of the intercondylar area. The posterolateral bundle (*black arrows*) comprises a more loosely arranged conglomeration of ligament fibres separated by fatty-type tissue and originates from the posterolateral aspect of the intercondylar area. *LTC* Lateral tibial condyle, *MFC* medial femoral condyle. *Asterisk* indicates the iliotibial band. **b** Oblique axial anatomical section from cadaveric knee showing anteromedial (*white arrows*) and posterolateral (*black arrows*) bundles near the tibial insertion. *Broken line* shows the demarcation between the two bundles. **c** Schematic drawing of the anteromedial and posterolateral bundles of the anterior cruciate ligament at the tibial insertion on oblique axial image. *AM* Anteromedial bundle, *PL* posterolateral bundle

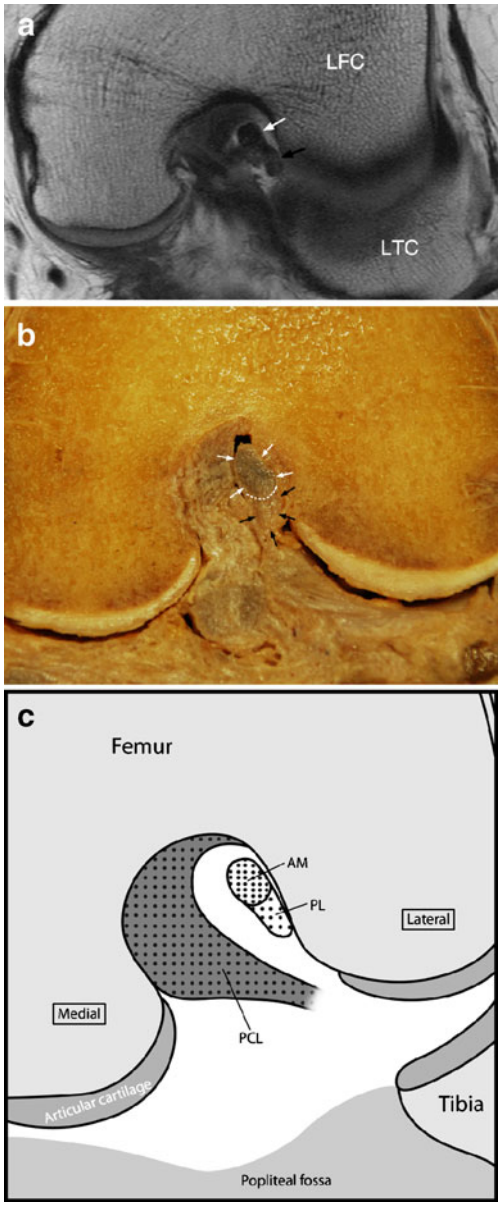

Fig. 4 **a** Oblique intermediate-weighted axial imaging at the mid-portion of the ACL in a volunteer. At this level, both bundles become more rounded and more compact in appearance with no visible intervening fat-type tissue between the fibres or bundles. Nevertheless both bundles remain distinguishable as quite discrete nodular masses located anteromedially and posterolaterally. *LFC* Lateral femoral condyle, *LTC* lateral tibial condyle. Anteromedial bundle (*white arrow*). Posterolateral bundle (*black arrow*). **b** Oblique axial anatomical section from cadaveric knee showing anteromedial (*white arrows*) and posterolateral (*black arrows*) bundles at the mid-portion of the ACL. *Broken line* shows the demarcation between the two bundles. **c** Schematic drawing of the anteromedial and posterolateral bundles of the anterior cruciate ligament at the mid-portion on oblique axial image. *AM* Anteromedial bundle, *PL* posterolateral bundle, *PCL* posterior cruciate ligament

1. A larger central area of hyperintensity at the tibial and mid-portion of the anteromedial bundle was seen in 3 (5%) of 60 knees examined (Fig. 6a). The cause of this signal is uncertain but may represent mucoid degeneration or fibrofatty tissue.
2. An intermediate bundle was seen in 3 (5%) of 60 knees examined being clearly seen as a separate structure close to the tibial insertion although not identifiable as a separate structure at the mid-portion of the ACL or close to the femoral origin (Fig. 6b).
3. A ligamentum mucosum (i.e., inferior synovial plica) was seen in 1 (2%) of 60 knees examined (Fig. 6c).
4. A moderately attenuated posterolateral bundle throughout the length of the ACL was seen in 1 (2%) of 60 knees examined (Fig. 6d).
5. Small ganglion cysts were found in 3 (5%) of 60 knees examined. One cyst was located in the anteromedial bundle, one in the posterolateral bundle, and one in both bundles (Fig. 2d).

Delineation of ACL bundles on MR imaging

The two bundles could be delineated in all cases. The ability to delineate both bundles of the ACL on oblique axial and standard sagittal, coronal, and axial images is shown in Table 1. After combining all three assessment areas (near tibial insertion, mid-portion, or near femoral origin), either good or adequate delineation of both bundles was apparent in 99% (178 of 180 areas assessed) on oblique axial imaging compared to 43% on standard sagittal, 47% on standard coronal, and 39% on standard axial images. For all areas, bundle delineation was better on oblique axial imaging than sagittal, coronal, or axial imaging ($P < 0.0001$ for all levels) (Table 1). Delineation of both ACL bundles was particularly poor close to the femoral attachment on sagittal, coronal, and axial imaging (Table 1).

Interreader reliability of ACL bundle delineation

Substantial agreement was found between both observers regarding the delineation of the ACL bundles on oblique axial and standard sagittal, coronal, and axial imaging at tibial insertion (k=0.62), mid portion (k=0.80), and femoral origin (k=0.73). The overall agreement was also substantial (k=0.75).

Discussion

Both bundles of the ACL, which are named according to their tibial insertion, are comparable in size and consistency [3, 17]. Both bundles attach to the medial aspect of the lateral femoral condyle proximally and to the anteromedial aspect of the tibial intercondylar area distally [3, 18].

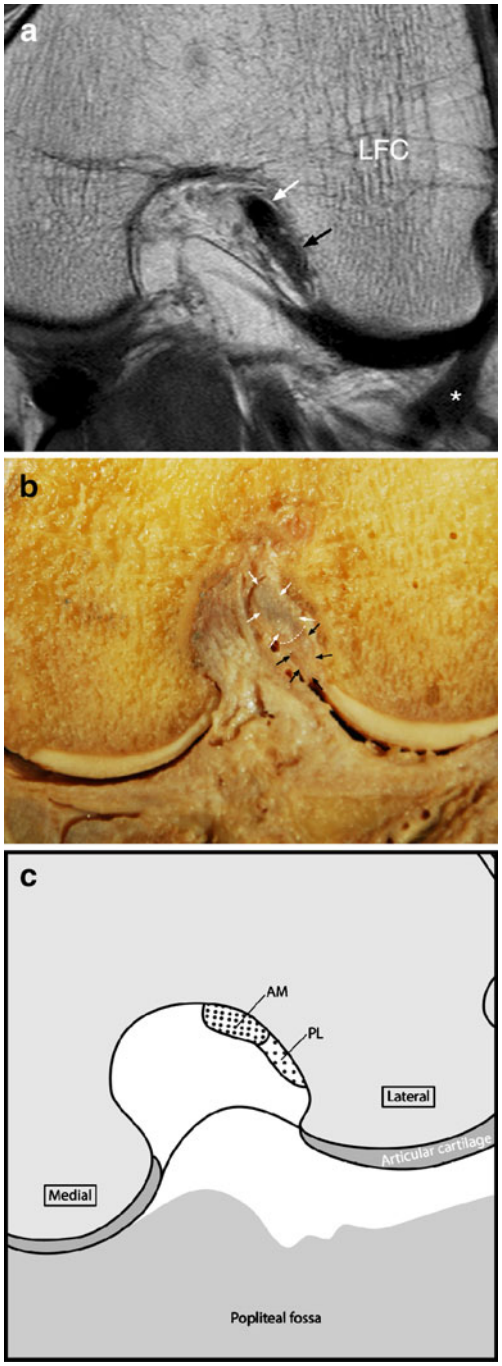

◀ **Fig. 5** **a** Oblique intermediate-weighted axial imaging of ACL near the femoral insertion in a volunteer. The anteromedial bundle (*white arrow*) is attached more anteriorly and medially than the posterolateral bundle (*black arrow*). At this location, both bundles are more oblong in contour with the anteromedial bundle being uniformly hypointense and the posterolateral bundle slightly less hypointense. Both bundles are of similar size and contact each other but can be distinguished by their location and different signal intensities. *LFC* Lateral femoral condyle. *Asterisk* indicates popliteus tendon. **b** Oblique axial anatomical section from cadaveric knee showing anteromedial (*white arrows*) and posterolateral (*black arrows*) bundles near the femoral attachment. *Broken line* shows the demarcation between the two bundles. **c** Schematic drawing of the anteromedial and posterolateral bundles of the anterior cruciate ligament at the femoral origin on oblique axial image. *AM* Anteromedial bundle, *PL* posterolateral bundle

Occasionally, an intermediate bundle may be found located between the anteromedial and posterolateral bundles [1, 4].

Clear separation of the two ACL bundles is limited on routine MR imaging by their close proximity, oblique orientation, and partial volume averaging [5, 19]. Only a few studies have addressed ACL bundle anatomy on MR imaging. The length of each bundle was measured on sagittal MR imaging although this particular study did not assess how well each bundle could be seen [10]. In a separate study of six cadaveric knees, the ACL bundles were found to be broadly recognizable on oblique sagittal and coronal planes at 3 T [20]. Kaya et al. studied 64 patients and found that combined analysis of standard sagittal, coronal, and axial MR imaging at 1.5 T allowed depiction of normal ACL bundle structure in only 42% of cases [11]. In a study primarily addressing partial tears of the ACL, Roychowdhury et al. described the appearances of the normal ACL on true axial imaging. They found wide variability in the shape of the ACL at the tibial insertion with the mid- to proximal portion of the ACL tending to be of smooth ellipse or oval configuration. This study also first described the "isolated ACL bundle sign" as a sign of partial ACL tear [19].

Casagranda et al. studied double bundle ACL grafts and found oblique coronal imaging useful when assessing integrity of the ACL bundles [21]. The current study is the first to use an oblique axial plane to visualize the ACL on MR imaging and also the first in-vivo 3 T MR study to comparatively analyze delineation of the ACL bundles.

Technically, the oblique axial plane is easy to acquire and does not require any knee repositioning unlike imaging in flexion which is also useful for improving ACL ligament conspicuity [22–24]. A clear potential benefit of imaging in an oblique axial plane is that it allows the ACL to be visualized on 11–15 contiguous images rather than on 2–3 contiguous images as with sagittal or coronal imaging. As the bundles of the ACL run largely parallel to each other, oblique axial imaging planned from both the coronal and sagittal planes ensures that both bundles are imaged in a near transverse plane thereby minimizing likelihood of partial volume averaging.

In this study we compared the delineation of both ACL bundles near the tibial insertion, at the mid-third of the ACL, and near the femoral origin in the oblique axial plane with sagittal, coronal, and axial views. Oblique axial plane imaging of the ACL yielded significantly better delineation of both ACL bundles compared to standard sagittal, coronal, and axial imaging. Delineation of both ACL bundles on oblique axial imaging was good or adequate in 99% of areas assessed compared with 43% on sagittal, 47% on coronal, and 39% on axial imaging. The majority

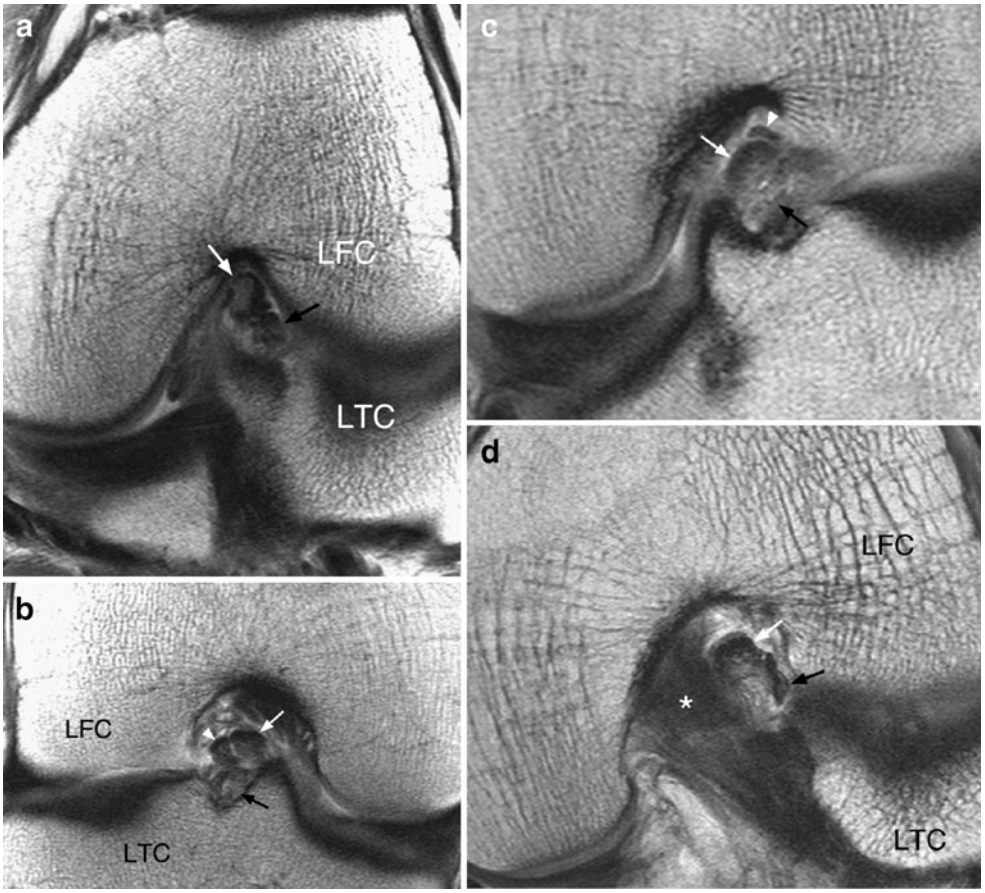

Fig. 6 Atypical appearances seen on intermediate-weighted oblique axial imaging of the ACL in subjects with no history of ACL injury or trauma. **a** At the mid-portion of the ACL, a central area of hyperintensity (*white arrow*) within the anteromedial bundle. **b** Near the tibial insertion, an intermediate bundle (*white arrowhead*) is present between the anteromedial (*white arrow*) and posterolateral bundles (*black arrow*). **c** Near the tibial insertion, an additional ligament-like structure (*white arrowhead*) extending from the tibial to the femoral attachment consistent with a ligamentum mucosum (inferior synovial plica). **d** At the mid-portion of the ACL, moderate attenuation of the posterolateral bundle (*black arrow*) is present while the anteromedial bundle (*white arrow*) is less hypointense and less well-defined and roundish than usual. Both bundles usually are of comparable size. *LFC* Lateral femoral condyle, *LTC* lateral tibial condyle. *Asterisk* indicates posterior cruciate ligament

of ACL tears tend to occur near the femoral origin [25], an area where both ACL bundles are particularly poorly delineated on sagittal, coronal, and axial imaging due to obliquity and close proximity of the ACL bundles. Yet this was an area in which bundle delineation remained consistently high on oblique axial imaging. Although not addressed in this study, clearer delineation of the ACL bundles may well allow improved recognition of partial tears and in this respect, awareness of the normal variants of the ACL bundles on oblique axial imaging would be helpful.

Atypical findings were present in only a small number of subjects. These included an intermediate bundle located between the anteromedial and posterolateral bundles close to the tibial insertion [4]. Other findings included a ligamentum mucosum, an increased hyperintensity of the

Table 1 Delineation of anteromedial and posterolateral ACL bundles on oblique axial and standard sagittal and coronal imaging. Comparisons were made at the tibial insertion, at the mid-portion, and at the femoral origin of the ACL. The delineation of the two bundles was graded as good, adequate, or poor. Differences in delineation of both bundles between the oblique axial and standard sagittal, coronal, and axial planes were highly significant ($P<0.0001$) at all levels

		Good delineation	Adequate delineation	Poor delineation
Tibial insertion	Oblique axial	40 (60%)	20 (40%)	0
	Standard sagittal	18 (30%)	25 (41.7%)	17 (28.3%)
	Standard coronal	17 (28.3%)	37 (61.7%)	6 (10%)
	Standard axial	16 (26.7%)	18 (30%)	26 (43.3%)
Mid-portion	Oblique axial	32 (53.3%)	28 (46.7%)	0
	Standard sagittal	7 (11.7%)	24 (40%)	29 (48.3%)
	Standard coronal	4 (6.7%)	12 (20%)	44 (73.3%)
	Standard axial	6 (10%)	10 (16.7%)	44 (73.3%)
Femoral origin	Oblique axial	31 (51.7%)	27 (45%)	2 (3.3%)
	Standard sagittal	1 (1.7%)	3 (5%)	56 (93.3%)
	Standard coronal	2 (3.3%)	12 (20%)	46 (76.7%)
	Standard axial	5 (8.3%)	15 (25%)	40 (66.7%)

anteromedial bundle close to the tibial insertion, a moderately attenuated posterolateral bundle, and small ACL ganglion cysts.

There were limitations to this study. First, oblique axial images were compared to sagittal, coronal, and axial imaging as has been used in previous studies to delineate both bundles [10]. We did not compare oblique axial imaging with oblique sagittal and oblique coronal. A further study comparing with oblique coronal and sagittal imaging would be useful. Second, we studied the ACL bundles only on intermediate-weighted oblique axial imaging. An intermediate-weighted sequence was employed as intermediate-weighted imaging is the most commonly used sequence to visualize the ACL [12, 19, 20, 24–26]. Third, as in other vivo studies with normal subjects, no arthroscopic correlation was possible as the knees included in this study were either clinically normal or had no knee symptoms related to ACL. Finally, no patients with knee trauma were included and as such the value of oblique axial imaging in detecting ACL injury was not assessed.

In conclusion, oblique axial intermediate-weighted imaging of the ACL improved visualization of the ACL bundles compared to sagittal, coronal, and axial imaging allowing both bundles to be clearly identified in the majority of cases. Further study in patients with knee trauma is required to determine if this imaging sequence also improves detection and localization of partial ACL tears.

Acknowledgements The work described in this paper was partially supported by a grant from the Research Grants Council of the Hong Kong Special Administrative Region, China (Project No.SEG_CUHK02).

Conflict of interest statement The authors declare that they have no conflict of interest.

References

1. Amis AA, Dawkins GP. Functional anatomy of the anterior cruciate ligament. Fibre bundle actions related to ligament replacements and injuries. J Bone Joint Surg Br. 1991;73:260–7.
2. Girgis FG, Marshall JL, Monajem A. The cruciate ligaments of the knee joint. Anatomical, functional, and experimental analysis. Clin Orthop Relat Res. 1975;106:216–31.
3. Fuss FK. Anatomy of the cruciate ligaments and their function in extension and flexion of the human knee joint. Am J Anat. 1989;184:165–76.
4. Norwood LA, Cross MJ. Anterior cruciate ligament: functional anatomy of its bundles in rotatory instabilities. Am J Sports Med. 1979;7:23–6.
5. Umans H, Wimpfheimer O, Haramati N, Applbaum YH, Adler M, Bosco J. Diagnosis of partial tears of the anterior cruciate ligament of the knee: value of MR imaging. AJR Am J Roentgenol. 1995;165:893–7.
6. Noyes FR, Mooar LA, Moorman 3rd CT, McGinniss GH. Partial tears of the anterior cruciate ligament. Progression to complete ligament deficiency. J Bone Joint Surg Br. 1989;71:825–33.
7. Sommerlath K, Odensten M, Lysholm J. The late course of acute partial anterior cruciate ligament tears. A nine to 15-year follow-up evaluation. Clin Orthop Relat Res. 1992;281:152–8.
8. Siebold R, Fu FH. Assessment and augmentation of symptomatic anteromedial or posterolateral bundle tears of the anterior cruciate ligament. Arthroscopy. 2008;24:1289–98.
9. Ochi M, Adachi N, Deie M, Kanaya A. Anterior cruciate ligament augmentation procedure with a 1-incision technique: anteromedial bundle or posterolateral bundle reconstruction. Arthroscopy. 2006;22:463.e1–5.
10. Cohen SB, VanBeek C, Starman JS, Armfield D, Irrgang JJ, Fu FH. MRI measurement of the 2 bundles of the normal anterior cruciate ligament. Orthopedics 2009 Sep;32(9).
11. Kaya A, Karadağ D, Güçlü B, Uçar F, Benli IT. Evaluation of the two bundles of the anterior cruciate ligament with 1.5 tesla magnetic resonance imaging. Acta Orthop Traumatol Turc. 2010;44:54–62.
12. Steckel H, Starman JS, Baums MH, Klinger HM, Schultz W, Fu FH. Anatomy of the anterior cruciate ligament double bundle structure: a macroscopic evaluation. Scand J Med Sci Sports. 2007;17:387–92.
13. Katahira K, Yamashita Y, Takahashi M, et al. MR imaging of the anterior cruciate ligament: value of thin slice direct oblique coronal technique. Radiat Med. 2001;19:1–7.
14. Hong SH, Choi JY, Lee GK, Choi JA, Chung HW, Kang HS. Grading of anterior cruciate ligament injury. Diagnostic efficacy of oblique coronal magnetic resonance imaging of the knee. J Comput Assist Tomogr. 2003;27:814–9.
15. Smith DK, May DA, Phillips P. MR imaging of the anterior cruciate ligament: frequency of discordant findings on sagittal-oblique images and correlation with arthroscopic findings. AJR Am J Roentgenol. 1996;166:411–3.
16. Cohen J. A coefficient of agreement for nominal scales. Educ Psychol Meas. 1960;20:37–46.
17. Harner CD, Baek GH, Vogrin TM, Carlin GJ, Kashiwaguchi S, Woo SL. Quantitative analysis of human cruciate ligament insertions. Arthroscopy. 1999;15:741–9.
18. Duc SR, Zanetti M, Kramer J, Käch KP, Zollikofer CL, Wentz KU. Magnetic resonance imaging of anterior cruciate ligament tears: evaluation of standard orthogonal and tailored paracoronal images. Acta Radiol. 2005;46:729–33.
19. Roychowdhury S, Fitzgerald SW, Sonin AH, Peduto AJ, Miller FH, Hoff FL. Using MR imaging to diagnose partial tears of the anterior cruciate ligament: value of axial images. AJR Am J Roentgenol. 1997;168:1487–91.
20. Steckel H, Vadala G, Davis D, Fu FH. 2D and 3D 3-tesla magnetic resonance imaging of the double bundle structure in anterior cruciate ligament anatomy. Knee Surg Sports Traumatol Arthrosc. 2006;14:1151–8.
21. Casagranda BC, Maxwell NJ, Kavanagh EC, et al. Normal appearance and complications of double-bundle and selective-bundle anterior cruciate ligament reconstructions using optimal MRI techniques. AJR Am J Roentgenol. 2009;192:1407–15.
22. Pereira ER, Ryu KN, Ahn JM, Kayser F, Bielecki D, Resnick D. Evaluation of the anterior cruciate ligament of the knee: comparison between partial flexion true sagittal and extension sagittal oblique positions during MR imaging. Clin Radiol. 1998;53:574–8.
23. Niitsu M, Ikeda K, Fukubayashi T, Anno I, Itai Y. Knee extension and flexion: MR delineation of normal and torn anterior cruciate ligaments. J Comput Assist Tomogr. 1996;20:322–7.
24. Remer EM, Fitzgerald SW, Friedman H, Rogers LF, Hendrix RW, Schafer MF. Anterior cruciate ligament injury: MR imaging diagnosis and patterns of injury. Radiographics. 1992;12:901–15.
25. Murakami Y, Sumen Y, Ochi M, Fujimoto E, Adachi N, Ikuta Y. MR evaluation of human anterior cruciate ligament autograft on oblique axial imaging. J Comput Assist Tomogr. 1998;22:270–5.
26. Kwon JW, Yoon YC, Kim YN, Ahn JH, Choe BK. Which oblique plane is more helpful in diagnosing an anterior cruciate ligament tear? Clin Radiol. 2009;64:291–7.